1990ApJ...354..708S

THE ASTROPHYSICAL JOURNAL, 354:708–719, 1990 May 10
© 1990. The American Astronomical Society. All rights reserved. Printed in U.S.A.

V795 HERCULIS (PG 1711+336): A NEW INTERMEDIATE POLAR IN THE PERIOD GAP

ALLEN W. SHAFTER AND EDWARD L. ROBINSON
McDonald Observatory and Department of Astronomy, The University of Texas at Austin
DAVID CRAMPTON
Dominion Astrophysical Observatory
BRIAN WARNER
Department of Astronomy, University of Cape Town; and Department of Astronomy, Dartmouth College
AND
RICHARD M. PRESTAGE
Steward Observatory, University of Arizona
Received 1989 August 25; accepted 1989 November 13

ABSTRACT

We report new photometric and spectroscopic observations of the nova-like variable V795 Her. The light curve has a periodic variation with a variable amplitude of roughly 25% peak-to-peak. Combining the new photometry with previously published photometry, we establish a period of 0.1164865(4) days for the variation. The emission lines in the spectrum display a radial velocity variation. We are unable to confirm the 0.6151 day period previously found for the radial velocities but we do find a period of 0.1082648(3) days with an amplitude of 70 ± 20 km s^{-1}. Our data establish conclusively that the photometric and spectroscopic periods are different. We argue that V795 Her is an intermediate polar and that one period is the orbital period and the other period is associated with the rotation of the magnetized, accreting white dwarf. We identify the spectroscopic period as the orbital period and suggest that the photometric period is the beat period between the orbital period and the rotation period of the white dwarf. The white dwarf could be rotating with a period of either 0.056108 or 0.073907 days, depending on whether radiation from one or both poles of the white dwarf is being reprocessed. The orbital period of V795 Her is near the middle of the gap in the orbital period distribution for cataclysmic variables. There are two possibilities for the evolutionary state of V795 Her. One possibility is that the secondary of V795 Her had such a low mass when the system was first formed in its precataclysmic state that the system did not achieve contact and begin mass transfer until its orbital period was less than 3 hr. Another possibility is that the mass transfer rate in V795 Her was low when its orbital period was near 3 hr. The secondary would, then, be nearer to thermal equilibrium and could survive to periods less than the upper edge of the period gap before losing contact, or it could reestablish contact at a period longer than the lower edge of the gap.

Subject headings: stars: binaries — stars: dwarf novae — stars: individual (V795 Her) — stars: white dwarfs

I. INTRODUCTION

During their search for faint objects with ultraviolet excesses at high galactic latitude, Green *et al.* (1982) identified V795 Her (PG 1711+336) as a possible cataclysmic variable based on its emission-line spectrum. Subsequent analysis of archival plates by Mironov, Moshkalev, and Shugarov (1983) showed that V795 Her exhibits slow brightness variations in the range $13.2 < B < 12.5$ with no evidence for dwarf nova eruptions. Mironov, Moshkalev, and Shugarov also found a periodic variation in the light curve with an amplitude of about 0.2 mag and a period of 0.115883 days with a possible alias at 0.131117 days. Later observations by Baidak *et al.* (1985) suggested a slightly different value of 0.114488 days for the photometric period. Baidak *et al.* noted that if this period is similar to the orbital period of the system, V795 Her is in the gap in the distribution of orbital periods of cataclysmic variables (Whyte and Eggleton 1980; Robinson 1983).

Thorstensen (1986) obtained time-resolved spectroscopic observations of V795 Her to look for evidence of orbital motion. Surprisingly, Thorstensen found no evidence for radial velocity variations of the Hα emission with a period anywhere near the photometric period. Instead, his data suggested a period of about 0.6151 days. This result led Thorstensen to suggest that V795 Her might be intermediate polar with an orbital period of 0.6151 days and that the photometric period might be caused by rotation of an accreting magnetized white dwarf in the system.

We independently began a program of spectroscopic observations of V795 Her in 1985, but after Thorstensen's results were published we decided that further photometric and spectroscopic observations were necessary to test the intermediate polar model and the spectroscopic period. Consequently, we obtained additional data in the spring and summer of 1986. We have already published a preliminary report of our results (Shafter *et al.* 1987). Our photometry revealed a period of 0.1164 days, slightly different from the previously published photometric periods. The dominant period in our spectroscopic data was at a period of $\sim$0.108 days, but one cycle per day aliases at $\sim$0.097 and $\sim$0.121 days could not be positively excluded. Although we found no evidence for Thorstensen's longer period, the intermediate polar hypothesis remained viable because our photometric period was not consistent with the dominant spectroscopic period or its aliases.

Recently, Rosen *et al.* (1988) published a photometric and spectroscopic study of V795 Her. They found two possible photometric periods, 0.1157550 and 0.1158807 days, which are

© American Astronomical Society • Provided by the NASA Astrophysics Data System

1990ApJ...354..708S

TABLE 1

PHOTOMETRIC OBSERVATIONS OF PG 1711+336

Run Number	Julian Date	Telescope (m)	PMT Tube	Integration Time (s)	Length of Run (hr)
69	2,446,172.9	2.1	RCA 8850	6.0	0.71
77	2,446,176.8	2.1	RCA 8850	5.0	2.83
79	2,446,177.9	2.1	RCA 8850	6.0	1.34
85	2,446,200.8	2.1	RCA 8850	5.0	3.00
N001	2,446,588.8	1.5	RCA C31034A	4.0	4.06
N003	2,446,589.8	1.5	RCA C31034A	4.0	4.34
N004	2,446,590.7	1.5	RCA C31034A	4.0	2.77
N010	2,446,593.7	1.5	RCA C31034A	4.0	3.02

close to but not the same as our value. In addition, they were able to confirm our discovery of radial velocity variations near the photometric period. However, because Rosen *et al.* had only ~3.3 hr of spectroscopic data, the precision of their period determination was insufficient to allow quantitative comparison with their photometric period. Furthermore, their limited spectroscopy precluded a search for low-frequency modulations near that found by Thorstensen (1986).

In this paper, we present all our data on V795 Her, including additional spectroscopy obtained in 1988 June. These data, taken together, suggest strongly that the orbital period of V795 Her is 0.108264 days (2.6 hr) and establish conclusively that the photometric and spectroscopic periods are indeed distinct. The most straightforward interpretation is that V795 Her is a member of the intermediate polar subclass of the cataclysmic variables.

II. OBSERVATIONS

a) Photometry

The new photometric observations consist of high-speed photometry obtained in two sets of four runs, one set in 1985 April and May and the other in 1986 June. The 1985 observations were obtained at McDonald Observatory with the 2.1 m telescope using the McDonald Observatory high-speed photometer (Nather 1973). The observations were made in unfiltered light with a blue-sensitive photomultiplier tube (an RCA 8850). The 1986 observations were obtained at McGraw Hill Observatory with the 1.5 m telescope using a standard photometer modified for high-speed photometry. The McGraw-Hill observations were made in unfiltered light with a red-sensitive RCA C31034A photomultiplier tube. Details about the individual runs are given in Table 1.

Two light curves from 1985 and two light curves from 1986 are shown in Figures 1–4. The star flickers actively on time scales as short as 1 minute and with amplitudes up to 20% peak-to-peak. Flickering is typical of all cataclysmic variables and in this regard V795 Her is normal, but the character of the flickering in V795 Her is unusual because the flickers are more clearly separated from their neighboring flickers. The flickering is aperiodic. We have calculated power spectra of all the data and find no significant enhancements of power at any periods between the Nyquist period (typically 8 s) and 1 hr, except for a slow rise in power toward low frequencies.

The light curve is strongly modulated at a period of roughly 3 hr. The amplitude of the modulation varies markedly from cycle to cycle but averaged about 25% peak-to-peak in 1985 data and slightly less, about 20%, in 1986 data. In the 1985 data, the light curve had a rapid rise and slower decay similar to the light curve found by Mironov, Moshkalev, and Shugarov (1983) and by Baidak *et al.* (1985). In the 1986 data, the variation was more symmetrical. The morphology of the light curve is, therefore, variable.

The published ephemerides for the photometric period of V795 Her are not in agreement. Mironov, Moshkalev, and Shugarov (1983) give $P = 0.115883$ days, Baidak *et al.* (1985) give $P = 0.114488$ days, Rosen *et al.* (1989) give $P = 0.11575498$ and 0.11588066 days, Kaluzny (1989) gives $P = 0.1166728$ days, and none of these photometric periods agree with the much longer spectroscopic period published by Thorstensen (1986). Our data show that none of these periods are correct.

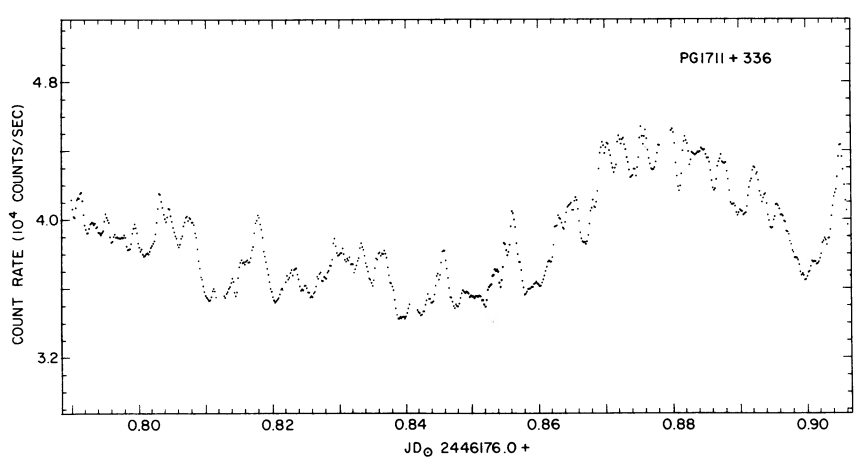

FIG. 1.—A high-speed photoelectric light curve of V795 Her from 1985

© American Astronomical Society • Provided by the NASA Astrophysics Data System

1990ApJ...354..708S

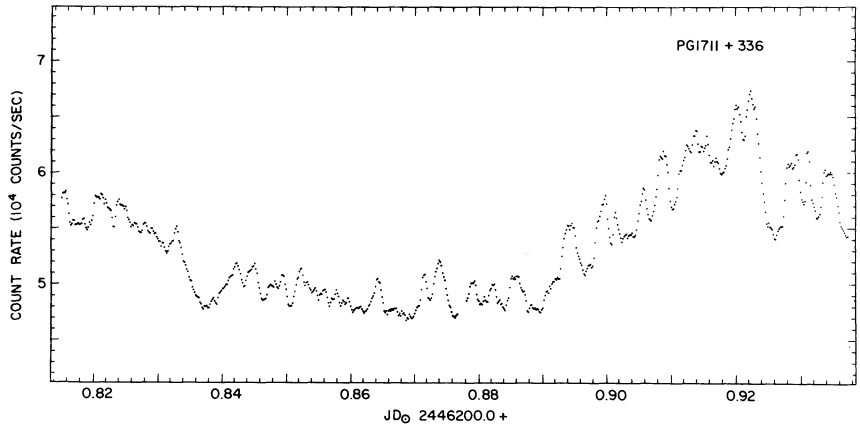

FIG. 2.—A high-speed photoelectric light curve of V795 Her from 1985

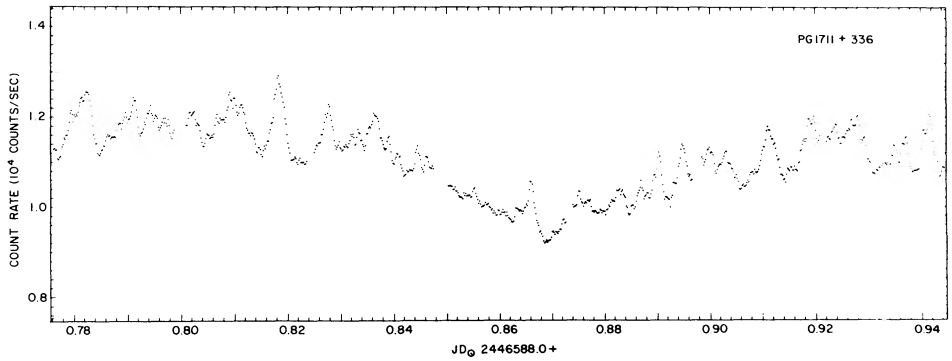

FIG. 3.—A high-speed photoelectric light curve of V795 Her from 1986

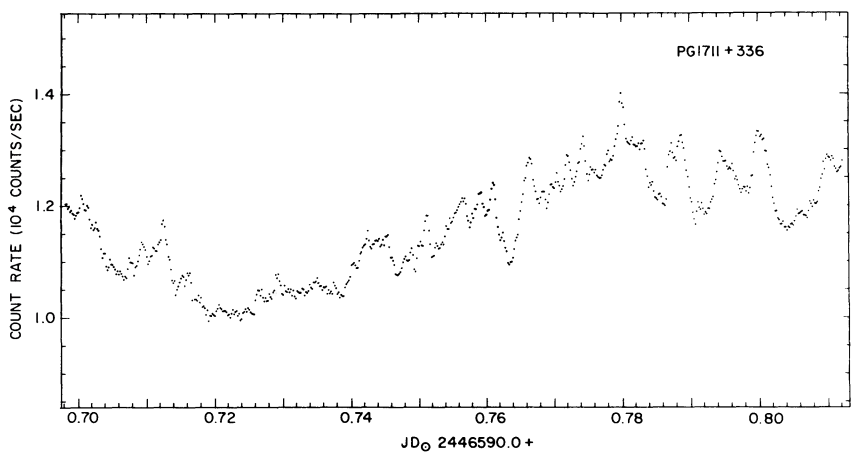

FIG. 4.—A high-speed photoelectric light curve of V795 Her from 1986

All times of minima that could be extracted from our light curves are given in Table 2. The variability of the light curves limits the accuracy of the times of minima to roughly ± 0.007 days. Based on our 1986 data alone, the only possible ephemeris for PG 1711 + 336 is

$$T_{\min} = \mathrm{JD}_\odot 2446588.867 + 0.1164E \,. \qquad (1)$$
$$\pm 1 \qquad \pm 3$$

This ephemeris is consistent with all published ephemerides except the one given by Baidak *et al.* (1985).

The ephemeris can be improved by including the timings of minima given by Rosen *et al.* (1989) and Kaluzny (1989), which are reproduced in Table 2. Rosen *et al.* (1989) made use of a time of minimum from Baidak *et al.* (1985). We do not use the Baidak *et al.* time of minimum because that time is really the zero point of their ephemeris, not a true time of minimum.

© American Astronomical Society • Provided by the NASA Astrophysics Data System

1990ApJ...354..708S

TABLE 2

TIMES OF PHOTOMETRIC MINIMA OF PG 1711+336

HJD (2,440,000.0+)	Cycle	O-C (Cycles)
5854.537[a]	−6264	0.03
5854.654[a]	−6263	0.04
5855.583[a]	−6255	0.01
6176.840[b]	−3497	−0.10
6200.871[b]	−3291	0.20
6280.513[a]	−2607	−0.10
6281.446[a]	−2599	−0.09
6588.869[b]	40	0.04
6589.795[b]	48	−0.01
6589.913[b]	49	0.01
6590.727[b]	56	−0.01
6593.756[b]	82	0.00
6939.725[c]	3052	0.03
6941.805[c]	3070	−0.11
6941.925[c]	3071	−0.08
6942.745[c]	3078	−0.04
6943.800[c]	3087	0.02
7307.821[c]	6212	0.02
7309.787[c]	6229	−0.10
7310.845[c]	6238	−0.02
7312.715[c]	6254	0.04
7312.835[c]	6255	0.07
7313.777[c]	6263	0.15
7313.874[c]	6264	−0.01

[a] Times from Rosen *et al.* 1989.
[b] Times from new photometry.
[c] Times from Kaluzny 1989.

Since the period found by Baidak *et al.* is incorrect, the zero point of the ephemeris can be different from a true time of minimum. With this larger data set, the linear ephemeris is uniquely determined:

$$T_{\min} = \mathrm{JD}_{\odot}\underset{\pm 2}{2446584.204} + \underset{\pm 4}{0.1164865}E\ . \qquad (2)$$

This ephemeris is different from all previously published ephemerides. The previous ephemerides appear to be aliases of the true ephemeris, differing from the true ephemeris by one or more cycles in several months. The *O-C* diagram corresponding to the ephemeris given in equation (2) is shown in Figure 5.

Two quadratic ephemerides are also consistent with the available times of minima, one with an increasing period $\dot{P} = 2.7 \times 10^{-8}$ and one with a decreasing period $\dot{P} = -1.7 \times 10^{-8}$. These are excessively large rates of change of the period and do not improve the residual scatter in the *O-C* diagram. Consequently, there is no compelling reason not to accept the constant-period ephemeris.

b) Spectroscopy

Our spectroscopic observations were obtained at the Dominion Astrophysical Observatory (DAO) in 1985 and 1986 and at the McDonald Observatory in 1986 and 1988. The DAO observations were obtained with the Cassegrain spectrograph of the 1.8 m reflector. The McDonald observations were made using the Cassegrain spectrographs of the 2.1 m reflector in 1986 and the 2.7 m reflector in 1988.

The DAO observations in 1985 were made with an intensified Reticon detector, while most of the 1986 data were obtained using a Shectograph. The Shectograph was used with an image slicer in exactly the same configuration as the intensified Reticon, so that the spectral resolutions for these two data sets were identical. Wavelength calibration spectra were taken immediately before and after every exposure. The FWHM of the comparison lines is approximately 1.7 Å. The spectra cover the wavelength region λλ4040–4920 and the signal-to-noise ratio of the spectra ranges from 13 to 28, depending largely on the seeing during the observations. The spectra were linearized in wavelength and the instrumental response was removed using the program "RETICENT" (Pritchet, Mochnacki, and Yang 1982).

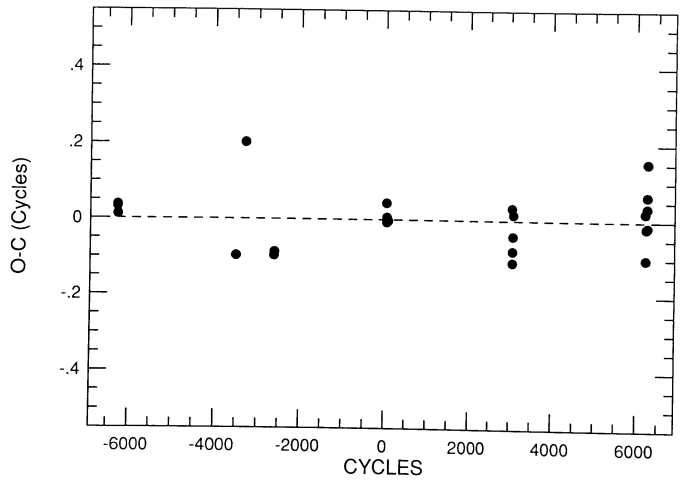

FIG. 5.—The *O-C* diagram for the photometric variation of V795 Her. The differences between the observed times of photometric minima and the calculated times of minima are plotted as a function of cycle number. The calculated times of minima are based on eq. (2). The standard deviation of the observed times of minima is ±0.007 days, most of which is caused by real changes in the shape of the light curve.

The McDonald data from 1986 were obtained using an RCA CCD having a readout noise of about 55 electrons. A 1200 lines mm^{-1} grating was used in first order resulting in a reciprocal dispersion of ~1.75 Å per pixel. With a typical slit width of 2″ (set by the seeing) the spectral resolution was ~3 Å FWHM. This configuration resulted in a wavelength coverage of about 900 Å, centered at roughly 4600 Å to cover Hγ, Hβ, and the He II λ4686 emission features.

The McDonald data from 1988 were obtained with a low readout noise (~15 electrons) TI CCD. Again a 1200 lines mm^{-1} grating was used, this time resulting in a reciprocal dispersion of ~0.9 Å per pixel because of the smaller 15 μ pixels. The typical spectral resolution was 2 Å FWHM over a wavelength range of λλ4250–4950. All individual McDonald integrations were bracketed by exposures of an argon arc-lamp to define the wavelength scale and assure velocity stability.

All exposure times were less than about 0.1 of the ~0.1 day photometric period. The DAO observations have exposure times of 15 minutes, while exposure times for the McDonald data were kept to 10 minutes. The details of our spectroscopic observations are summarized in Table 3.

III. RADIAL VELOCITIES

We measured the radial velocities of the emission lines by convolving their line profiles with a template spectrum consisting of two Gaussians whose width is much narrower than the width of the line (Shafter 1985; Shafter, Szkody, and Thorstensen 1986). The template is positioned so that one Gaussian is in the blue wing of the emission line and the other is in the red

© American Astronomical Society • Provided by the NASA Astrophysics Data System

1990ApJ...354..708S

TABLE 3

SPECTROSCOPIC OBSERVATIONS OF PG 1711+336

HJD (2,440,000.0+)	Observer	Telescope	Integration Time (minutes)	Number of Spectra	Relation (Å)
6264	L.W.	DAO 1.8 m	15	2	1.7
6292	D.C.	DAO 1.8 m	15	7	1.7
6293	L.W.	DAO 1.8 m	15	12	1.7
6296	D.C.	DAO 1.8 m	15	14	1.7
6560	A.W.S./E.L.R.	McD 2.1 m	10	23	3.5
6561	A.W.S./E.L.R.	McD 2.1 m	10	23	3.5
6562	A.W.S./E.L.R.	McD 2.1 m	10	15	3.5
6564	A.W.S./E.L.R.	McD 2.1 m	10	25	3.5
6565	A.W.S./E.L.R.	McD 2.1 m	10	32	3.5
6566	A.W.S./E.L.R.	McD 2.1 m	10	15	3.5
6566	D.C.	DAO 1.8 m	15	10	1.7
6591	D.C.	DAO 1.8 m	15	10	1.7
6592	D.C.	DAO 1.8 m	15	11	1.7
6625	D.C.	DAO 1.8 m	15	14	1.7
6641	D.C.	DAO 1.8 m	15	16	1.7
6644	D.C.	DAO 1.8 m	15	7	1.7
7329	A.W.S.	McD 2.7 m	10	26	1.8
7330	A.W.S.	McD 2.7 m	10	31	1.8
7331	A.W.S.	McD 2.7 m	10	26	1.8

wing. The wavelength of the template is adjusted by Newton-Raphson iteration procedure until the fluxes through the two Gaussian bandpasses are equal. The wavelength of the midpoint of the Gaussians is then taken as the velocity of the emission line (see Schneider and Young 1980). This technique has the advantage that phase-dependent structure in the emission lines can be studied by repeating the measurements using a variety of separations for the Gaussians.

a) Determination of the Orbital Period

The preliminary velocity measurements were made using a Gaussian separation of 1000 km s^{-1} and a Gaussian width characterized by $\sigma = 400$ km s^{-1}. The choice of these values was made from a visual inspection of the emission line width and the signal-to-noise ratio of the data and is somewhat subjective. The choice of the Gaussian parameters is not, however, critical at this stage of the analysis. The velocity measurements are given in Table 4.

After measuring the 319 individual spectra, we search for the orbital period using the Press and Rybicki (1989) algorithm for the Lomb-Scargle periodogram (Lomb 1976; Scargle 1982). Initially, we analyzed the velocities from each year separately, giving three groups of velocities: the 1985 DAO data (group 1), the 1986 DAO and McDonald data (group 2), and the 1988 McDonald data (group 3). Because the group 1 velocities are scanty and noisy, the periodogram for these data did not reveal any preferred period. Periodograms for groups 2 and 3 were much more informative and are shown in Figures 6 and 7. One cycle per day aliases appear in both periodograms, but both periodograms strongly favor a frequency of ~ 9.24 days^{-1}. We adopt this as the true orbital frequency, noting that frequencies of ~ 10.23 and 8.23 days^{-1} cannot be ruled out absolutely. To improve the precision of the orbital period determination, we next combined the data from all three groups and computed a final periodogram centered on the favored frequency. The periodogram, which covers the 1 cycle per day aliases, is shown in Figure 8. The peak frequency corresponds to an orbital period of 0.1082468 days. Although there appears to be a weak low-frequency component in the periodogram, we find no evidence for radial velocity variations at the period of 0.6151 days reported by Thorstensen (1986).

To find preliminary estimates of the remaining orbital ele-

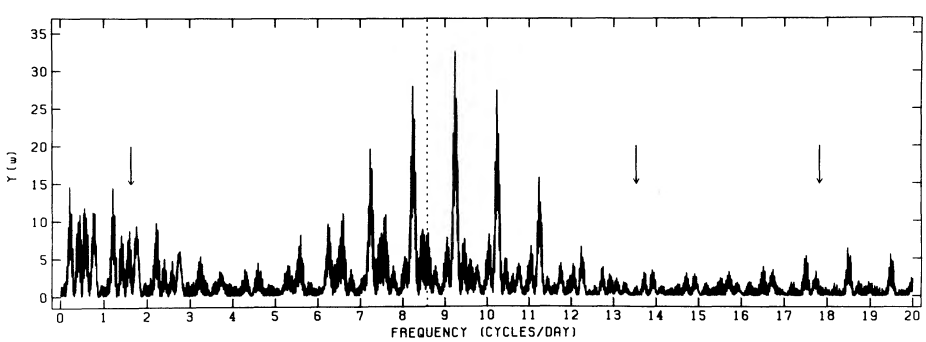

FIG. 6.—The Loam-Scargle periodogram for the 1986 (group 2) data. The most probable spectroscopic frequency is ~ 9.23 cycles per day. The dashed line is at the 0.1164865 day photometric period. The arrow at 1.62 days^{-1} shows the position where the previously reported 0.615 day period would be located if it were present. The other two arrows show the possible rotation frequencies of the white dwarf.

© American Astronomical Society • Provided by the NASA Astrophysics Data System

1990ApJ...354..708S

TABLE 4

RADIAL VELOCITIES

HJD (2,440,000+)	Velocity (km s^{-1})	HJD (2,440,000+)	Velocity (km s^{-1})	HJD (2,440,000+)	Velocity (km s^{-1})	HJD (2,440,000+)	Velocity (km s^{-1})
6264.810	−133	6561.827	−36	6565.856	−123	6625.900	51
6264.822	−241	6561.836	−34	6565.867	−130	6625.910	−26
6292.729	25	6561.843	−179	6565.875	−7	6625.922	−128
6292.739	−109	6561.852	−85	6565.882	22	6641.740	−8
6292.749	40	6561.859	−97	6565.891	29	6641.764	27
6292.832	−26	6561.867	9	6565.898	7	6641.777	−41
6292.843	−15	6561.875	137	6565.907	41	6641.789	−29
6292.853	50	6561.883	106	6565.914	27	6641.800	53
6292.864	11	6561.891	101	6565.922	−42	6641.812	44
6293.724	−86	6561.899	103	6565.930	−62	6641.825	−106
6293.737	−78	6561.907	122	6565.938	0	6641.838	−87
6293.747	71	6562.830	140	6565.946	−45	6641.850	−34
6293.760	68	6562.846	188	6565.954	−161	6641.862	−47
6293.772	79	6562.854	157	6566.709	−85	6641.874	−37
6293.783	10	6562.862	−16	6566.751	129	6641.886	−31
6293.794	48	6562.870	47	6566.762	63	6641.898	−8
6293.806	17	6562.878	147	6566.766	40	6641.911	1
6293.818	−26	6562.886	46	6566.770	216	6641.923	18
6293.829	−65	6562.894	51	6566.780	25	6641.935	−17
6293.841	5	6562.902	64	6566.786	15	6644.785	70
6293.853	−67	6562.909	−70	6566.793	86	6644.799	−43
6296.708	−7	6562.918	21	6566.795	38	6644.812	36
6296.718	31	6562.925	−56	6566.803	−8	6644.825	31
6296.729	−58	6562.933	−47	6566.807	7	6644.838	35
6296.739	21	6562.941	22	6566.811	−39	6644.851	−33
6296.750	−80	6562.949	137	6566.820	−96	6644.864	−127
6296.761	−3	6564.686	90	6566.820	−59	7329.708	8
6296.772	118	6564.695	82	6566.828	−5	7329.722	−53
6296.782	62	6564.702	48	6566.833	17	7329.730	−98
6296.793	108	6564.711	46	6566.835	106	7329.742	−101
6296.803	46	6564.719	−42	6566.844	84	7329.750	−107
6296.813	12	6564.727	46	6566.854	167	7329.761	−59
6296.823	−17	6564.735	−15	6566.863	82	7329.768	67
6296.833	26	6564.743	2	6566.867	7	7329.779	47
6296.843	43	6564.750	−9	6566.881	110	7329.788	34
6560.770	−100	6564.759	−133	6566.882	54	7329.799	6
6560.759	−173	6564.766	−67	6566.891	37	7329.807	11
6560.768	−158	6564.775	−94	6566.894	25	7329.818	74
6560.776	−260	6564.782	147	6591.756	24	7329.826	40
6560.787	3	6564.790	80	6591.773	165	7329.837	−9
6560.807	−33	6564.798	145	6591.786	109	7329.845	−103
6560.815	14	6564.806	114	6591.797	67	7329.855	−132
6560.825	25	6564.814	76	6591.808	6	7329.864	−85
6560.833	13	6564.822	130	6591.820	−79	7329.874	−122
6560.843	−43	6564.830	−4	6591.909	60	7329.882	−16
6560.850	−21	6564.838	65	6591.920	−41	7329.893	52
6560.860	−127	6564.845	−182	6591.932	24	7329.901	17
6560.868	−117	6564.854	−86	6591.944	−43	7329.912	−14
6560.877	−132	6564.861	−99	6592.762	−23	7329.922	25
6560.885	−63	6564.870	−133	6592.774	−29	7329.932	−14
6560.894	−25	6564.877	−293	6592.785	−44	7329.941	−33
6560.902	−38	6565.692	−37	6592.796	−81	7329.952	−70
6560.911	−94	6565.701	108	6592.808	−39	7330.644	−25
6560.919	21	6565.708	−0	6592.819	−16	7330.657	48
6560.928	−25	6565.716	−31	6592.896	−106	7330.664	31
6560.936	17	6565.726	−53	6592.909	−121	7330.675	52
6560.944	−124	6565.735	−49	6592.921	−91	7330.683	100
6560.952	15	6565.742	−116	6592.932	−6	7330.694	−8
6561.707	27	6565.750	−2	6592.943	16	7330.702	−41
6561.718	−30	6565.762	−76	6625.786	−32	7330.713	−122
6561.745	51	6565.770	28	6625.797	38	7330.721	−94
6561.754	83	6565.777	−44	6625.807	11	7330.731	−42
6561.762	144	6565.786	26	6625.818	−64	7330.741	−155
6561.770	137	6565.795	32	6625.828	−67	7330.752	69
6561.778	32	6565.803	47	6625.838	24	7330.760	73
6561.787	39	6565.814	11	6625.849	37	7330.771	56
6561.795	58	6565.824	−41	6625.859	−1	7330.780	75
6561.804	22	6565.832	−51	6625.869	51	7330.791	−15
6561.812	57	6565.840	−58	6625.880	7	7330.799	23
6561.820	75	6565.848	−69	6625.890	22	7330.809	−12

© American Astronomical Society • Provided by the NASA Astrophysics Data System

1990ApJ...354..708S

TABLE 4—*Continued*

HJD (2,440,000+)	Velocity (km s^{-1})	HJD (2,440,000+)	Velocity (km s^{-1})
7330.818.....	85	7331.768.....	4
7330.828.....	−116	7331.777.....	23
7330.837.....	−107	7331.788.....	−81
7330.848.....	31	7331.798.....	−80
7330.855.....	89	7331.808.....	−141
7330.866.....	125	7331.816.....	−15
7330.873.....	38	7331.827.....	73
7330.885.....	48	7331.835.....	19
7330.893.....	50	7331.846.....	104
7330.904.....	−7	7331.854.....	110
7330.912.....	−22	7331.866.....	86
7330.923.....	−38	7331.874.....	100
7330.930.....	1	7331.884.....	77
7331.702.....	−45	7331.893.....	−5
7331.713.....	17	7331.903.....	−89
7331.721.....	88	7331.911.....	−141
7331.731.....	101	7331.922.....	−92
7331.739.....	118	7331.929.....	55
7331.750.....	121	7331.940.....	179
7331.757.....	27		

ments, we fit the velocities with a sinusoid of the form:

$$V(t, s) = \gamma(s) - K(s) \sin \left\{ \frac{2\pi[t - T_0(s)]}{P} \right\},$$

where γ is the systemic velocity, K is the semiamplitude of the emission-line source, T_0 is the time of conjunction, P (= 0.01082648 days) is the orbital period, and s is the Gaussian separation, which we initially took to be 1000 km s^{-1}. The systemic velocity was not reliable, so we artificially shifted the mean of the velocities to zero. The fit yielded $K = 70(5)$ km s^{-1}, and $T_0 = \mathrm{JD}_{\odot}2{,}447{,}329.824(2)$. Figure 9 shows the fit to the data. The rms residual of the measurements about the best-fit sine curve is ± 48 km s^{-1}. The scatter is caused primarily by intrinsic variations of the star, not by measurement errors.

b) The Diagnostic Diagrams

In the absence of any phase-dependent line asymmetries, the values of the orbital elements should be independent of the line measuring technique. However, the emission lines seen in the spectra of cataclysmic variables typically have a complex structure with at least one component that is dependent on the orbital phase. A phase-dependent line asymmetry, such as an S-wave, makes the determination of certain orbital elements (e.g., velocity amplitudes and phases) difficult. Specifically, the values of these elements depend significantly on which portion of the emission-line profile is used in the velocity measurements.

If a phase-dependent line asymmetry is caused by emission from the region near the impact of the mass transfer stream and the outer disk (the bright spot), it is usually desirable to measure the velocities from the extreme line wings. The line wings are formed in the inner regions of the accretion disk, where the effect of the mass transfer stream should be minimal. To test this possibility and to explore the behavior of line asymmetries, we (Shafter 1985; Shafter, Szkody, and Thorstensen 1986) have found it useful to measure velocities for a variety of positions in the line profile (i.e., for a range of Gaussian separations). Orbital solutions based on velocity measurements for a given Gaussian separation are then plotted as a

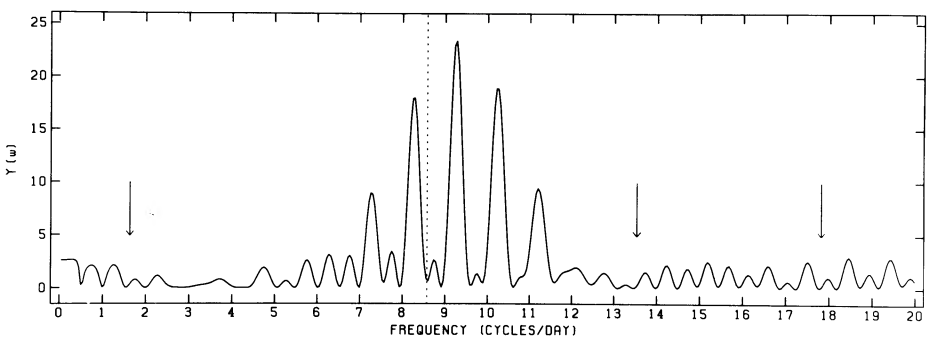

FIG. 7.—The periodogram for the 1988 (group 3) data. The most probable orbital frequency is clearly ~9.23 cycles per day. The dashed line is at the 0.1164865 day photometric period. The arrow at 1.62 days^{-1} shows the position where the previously reported 0.615 day period would be located if it were present. The other two arrows show the possible rotation frequencies of the white dwarf.

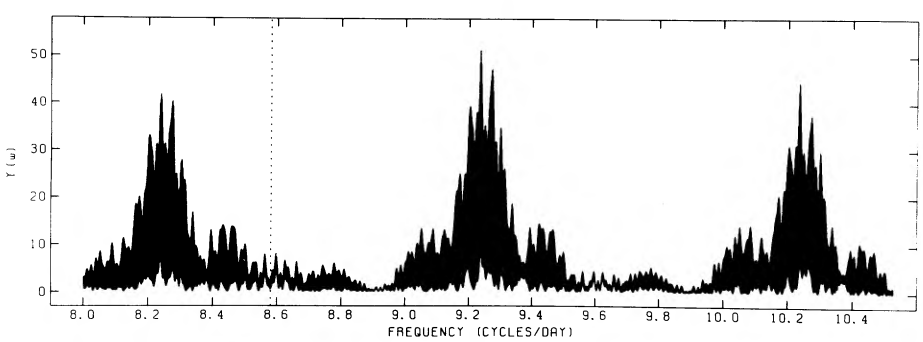

FIG. 8.—The total periodogram based on all our spectroscopic observations

© American Astronomical Society • Provided by the NASA Astrophysics Data System

1990ApJ...354..708S

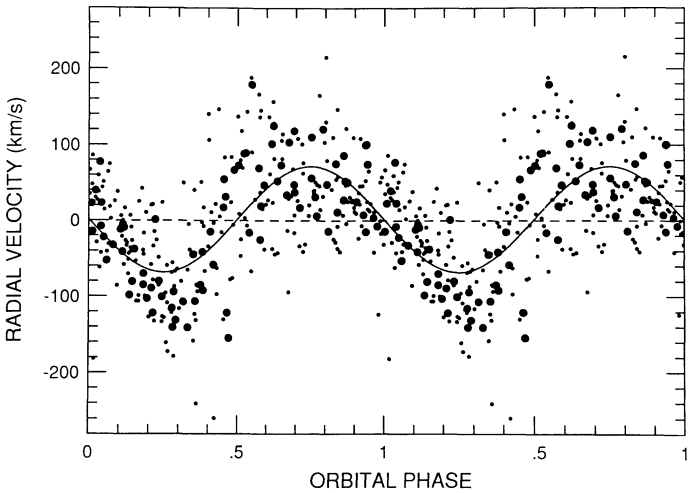

FIG. 9.—The radial velocity measurements from all 319 spectra folded with the 0.1082648 day orbital period and plotted as a function of orbital phase. The 1988 McDonald (group 3) velocities been given double weight and are shown as larger dots. The rms residual of the observed velocities about the fitted curve is ± 48 km s^{-1}. The scatter is caused by real changes in the line profiles, not by measurement error.

function of position in the line profile resulting in a "diagnostic diagram."

We began by co-adding the individual spectra into orbital phase bins to improve the signal-to-noise ratio. The spectra resulting from the co-addition are displayed in Figure 10. A phase-dependent asymmetry is clearly present. The lines are double-peaked with the violet-displaced peak strongest throughout most of the orbit and reaching a peak strength near orbital phase 0.5 (inferior conjunction of the emission line source). At this orbital phase, the side of the accretion disk that trails the white dwarf in its orbit is approaching the observer. Since the stream of mass from the companion star impacts the disk on the trailing side, it seems likely that the excess emission arises near the hot spot. In this respect, the phase-binned spectra exhibit the standard S-wave disturbance. It is, however, not obvious why the red peak is so weak near orbital phase zero. It is possible that emission from the hot spot may be partially obscured by the mass transfer stream during this part of the orbit.

The equivalent widths of the Hβ emission are plotted as a function of orbital phase in Figure 11. The equivalent width peaks twice during the orbit. Both peaks occur at quadrature (near orbital phases 0.25 and 0.75). Since the bright spot is most visible near phase 0.75, it seems plausible that the spot is responsible for the relatively large line strength observed at this phase. In a similar way, the excess emission near orbital phase 0.25 could be a result of reprocessed radiation from a raised rim of the disk near the bright spot.

Velocities based on the 12 coadded spectra have been measured for both the Hβ and He II emission features. All measurements were made with Gaussian bandpasses characterized by $\sigma = 250$ km s^{-1}. For the Hβ line, we included Gaussian separations, s, between 400 and 2200 km s^{-1} in 200 km s^{-1} intervals. We only extended the Gaussian separation to 1400 km s^{-1} for the He II line because greater separations risk contaminated by the C III–N III complex near 4650 Å. Orbital elements for each value of the Gaussian separation were determined by fitting a sine curve to the velocities as described in the previous section. The values of the orbital elements were then plotted as a function of the Gaussian separation, forming the diagnostic diagrams.

The diagnostic diagrams for Hβ and He II are shown in Figures 12 and 13. The velocity amplitude of the Hβ emission line lies between 60 and 90 km s^{-1}. The velocity amplitude of the He II line is somewhat smaller but is consistent with this range. The absolute scale for the γ-velocities is not reliable, because it was necessary to adjust the zero point of the spectra before combining the data from the different observing runs.

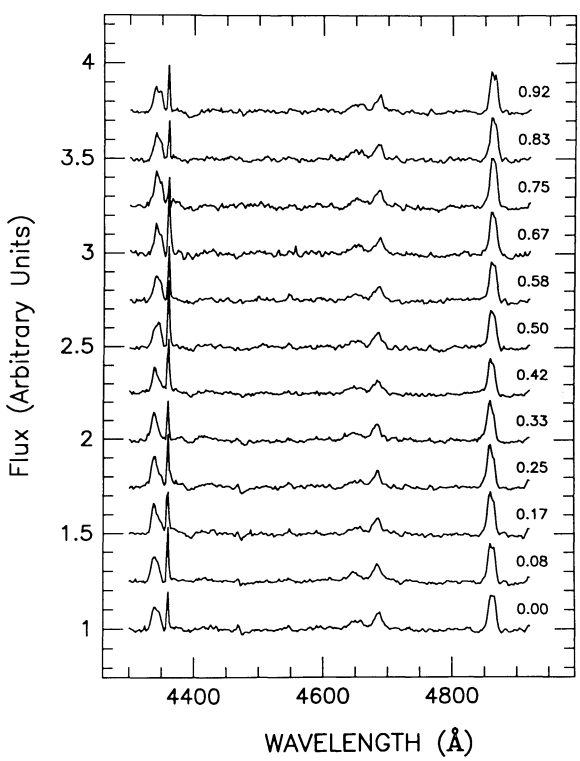

FIG. 10.—The 319 individual spectra have been folded with the orbital period and coadded into 12 orbital phase bins. The sharp line at λ4358 is a terrestrial mercury vapor line. Note the presence of a violet-displaced emission component which peaks near orbital phase 0.5.

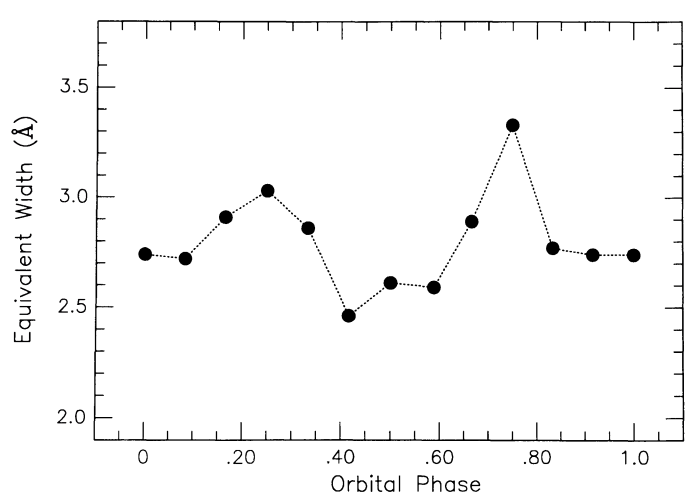

FIG. 11.—The variation of the equivalent width of Hβ with orbital phase

© American Astronomical Society • Provided by the NASA Astrophysics Data System

1990ApJ...354..708S

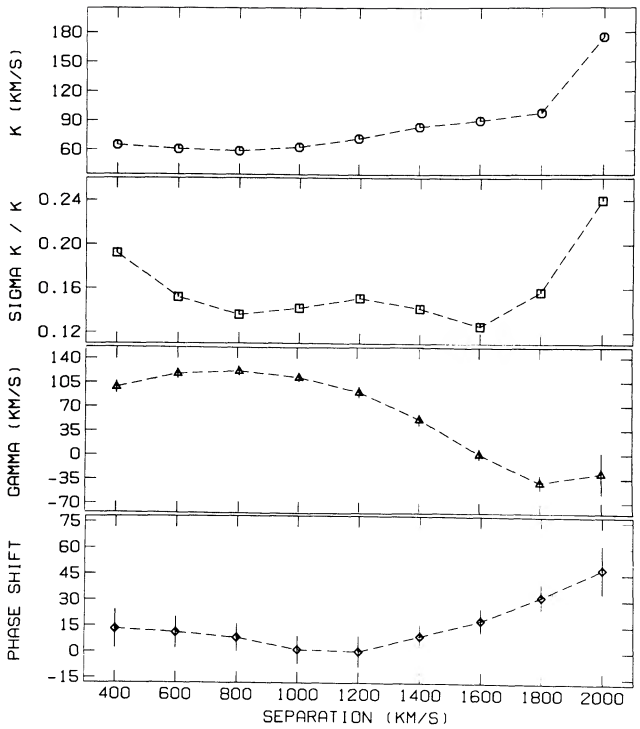

FIG. 12.—The diagnostic diagram for the Hβ line

Also, because V795 Her is not an eclipsing system, we have no way of knowing the true time of spectroscopic conjunction. Consequently, the phases shift has been computed relative to an arbitrary fiducial point. We have defined zero phase shift to be the phase for the measurement of the Hβ line using a Gaussian separation of 1200 km s^{-1}.

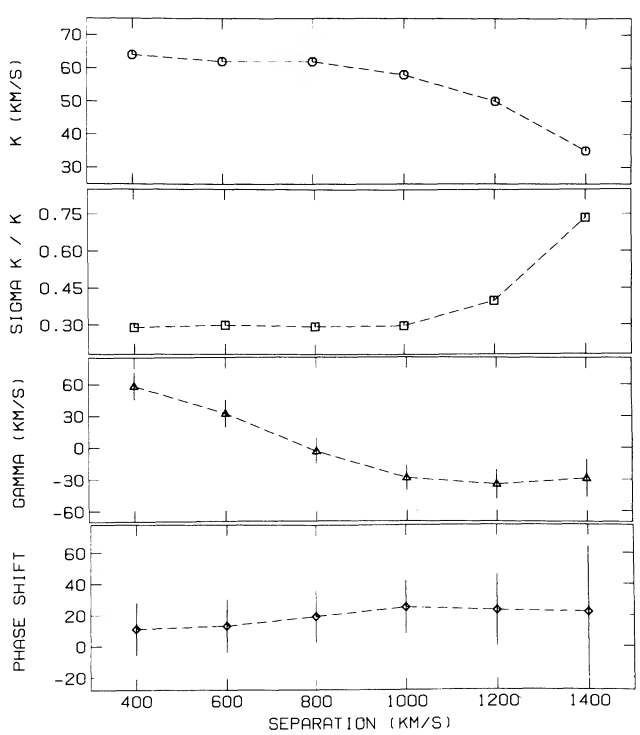

Fig. 13.—The diagnostic diagram for the He II line

TABLE 5

ORBITAL ELEMENTS OF V795 HERCULIS[a]

Element	Value
Photometric Period (days)	0.1164865(4)
Spectroscopic Period (days)	0.1082648(3)
T_0 (HJD)[b]	2,447,329.824(2)
K (km s^{-1})	70(20)

[a] Eccentricity assumed to be zero.
[b] Superior spectroscopic conjunction.

Although it is not possible to determine the absolute phase shift, the diagnostic diagrams do show that phase shifts of up to 0.15 are possible depending on which part of the line profile is used in the velocity measurements. Consequently, we will retain the value of T_0 determined previously with the cautionary note that the uncertainty may be as high as 0.02 days depending on which position in the line profile is used in the velocity measurements. The semiamplitude of the radial velocity variations is also not well constrained. It is clear from the diagnostic diagrams that our initial estimate of $K = 70$ km s^{-1} should have an uncertainty of roughly 20 km s^{-1} associated with it. The best estimates for the orbital elements of V795 Her are summarized in Table 5.

IV. DISCUSSION

a) The Spectrum

Nova-like variables generally have higher accretion rates than dwarf novae (Warner 1987, and references therein). The higher accretion rates increase the optical depth in the disk, increase the flux of continuous radiation and make the nova-like variables more luminous than the dwarf novae. The spectra of nova-like variables usually have weak He II and Balmer emission superposed on a strong blue continuum. The spectra of dwarf novae are characterized by strong Balmer emission and moderately strong He I emission. He II emission is absent or weak. The spectra of the magnetic cataclysmic variables are similar to those of the nova-like variables except that the He II emission in the magnetic systems is usually as strong or stronger than the Balmer emission. The strong He II emission is formed in the high-temperature shocked regions near the accreting magnetic poles of the white dwarf.

The sum of all our spectra of V795 Her is shown in Figure 14. The spectrum is similar to that of the nova-like variables. In particular, it is similar to the spectrum of KR Aur, a nova-like variable with a period of 0.163 days (Shafter 1983; Hutchings, Link, and Crampton 1983). The spectra of both systems have moderately strong Balmer emission, weak He II emission, and little or no He I emission. The weakness of the He II emission is peculiar because, as we will show in the next section, V795 Her is an intermediate polar.

Finally, we observed a weak and broad absorption feature to the blue of Hβ in several spectra we obtained in 1986. While we have no reason to believe the feature is spurious, there was no trace of it on any of our later spectra, most of which were of higher quality. The reality of this absorption is, therefore, uncertain.

b) The Intermediate Polar Model

We have established that the spectroscopic and photometric periods of V795 Her are different. This result is robust and would be unchanged even if we have chosen the incorrect

© American Astronomical Society • Provided by the NASA Astrophysics Data System

1990ApJ...354..708S

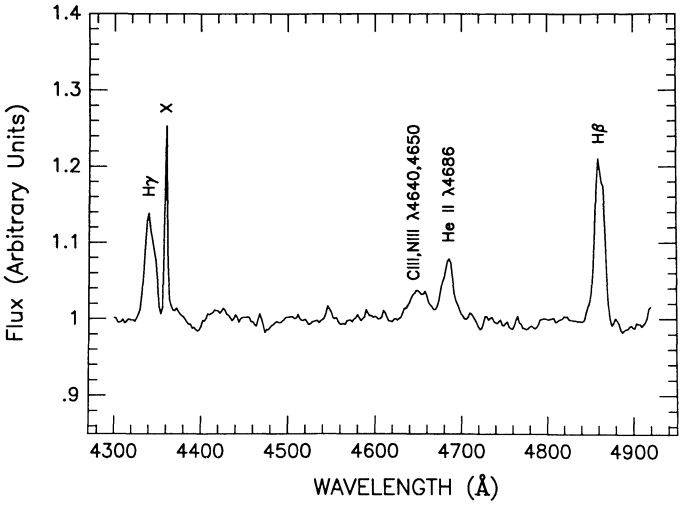

FIG. 14.—The mean of all of our spectroscopic observations. The sharp line at λ4358 is a terrestrial mercury vapor line.

aliases of either period. The preferred explanation for this behavior is that V795 Her is an intermediate polar. As for other intermediate polars, we identify the spectroscopic period with the orbital period and the photometric period with the spin period of an accreting magnetic white dwarf. There is one interesting complication to the model: In V795 Her, the photometric period is *longer* than the spectroscopic period. One expects that accretion torques should decrease the rotation period of the white dwarf until its period reaches an equilibrium value determined primarily by the mass accretion rate and the strength of the white dwarf's magnetic field. The rotation period of the white dwarf should, therefore, always be shorter than the orbital period of the binary. Indeed, the rotation periods of the white dwarfs in most intermediate polars are considerably less than the orbital period, the shortest being the rotation period of the white dwarf in AE Aqr, 33 s (Patterson 1979). Except for those magnetic systems in which the white dwarf rotation period is synchronously locked to the orbital period, the polars or AM Her stars, the white dwarf with the longest rotation period is in TT Ari. It rotates with a period of $P = 0.1329$ days (Mardirossian *et al.* 1980) only slightly shorter than the orbital period of the system, $P = 0.1375512$ days (Thorstensen, Smak, and Hessman 1985).

Since it is difficult to understand how the white dwarf could be rotating with a lower angular frequency than the binary, we propose that the photometric period is the beat period between the rotation of the white dwarf and the orbital period. If beamed X-ray radiation from the white dwarf is being reprocessed by the companion star and emitted as visible light, the rotation period of the white dwarf is given by:

$$\frac{1}{P_{\rm rot}} = \frac{1}{P_{\rm rep}} + \frac{1}{nP_{\rm orb}},$$

where $P_{\rm rot}$, $P_{\rm rep}$, and $P_{\rm orb}$ are the white dwarf rotation period, the reprocessing period, and the orbital period, respectively. For a single beam of X-rays, n equals 1 and for a dipole beam n equals 2. The rotation period of the white dwarf would then be 0.056108 days ($\sim$1.35 hr) for a single beam and 0.073907 days ($\sim$1.77 hr) for a dipole beam. There is no evidence for either of these periods in our data (see Figs. 6–8). One or the other should, however, be present at X-ray wavelengths.

If future X-ray or optical observations establish that the 0.1164 day photometric period is really the rotation period of the white dwarf, not the reprocessing period, we must be willing to consider the possibility that our preferred spectroscopic period is an alias of the true orbital period. Specifically, the alias period at 0.1214 days, which cannot be ruled out entirely by our observations, would be an acceptable orbital period. V795 Her would then be similar to TT Ari (Shafter *et al.* 1985; Thorstensen, Smak, and Hessman 1985).

It is puzzling that Thorstensen (1986) found no evidence for the 0.1082 day radial velocity variations that dominate our data. This has caused us to consider the (remote) possibility that the 0.1082 day period is not caused by orbital motion, but is simply a modulation of the emission-line profile. Such a modulation could be caused by a periodic heating of the surface of the accretion disk by beamed radiation from the magnetic poles of the white dwarf or, as in 1H0542−407, it could be caused by emission from a shocked region at the inner disk boundary corotating with the white dwarf (Buckley and Tuohy 1990). If the mass accretion rate during Thorstensen's observations was lower than the rate during our observations, the accretion-induced line profile variations may have been insignificant, allowing the orbital variations to show. If this is happening, the 0.6151 day period seen by Thorstensen (1986) could be the orbital period of the binary. There are, however, strong objections to this interpretation. First, it is difficult to accept that a secondary star filling its Roche lobe in a cataclysmic variable with a 15 hr orbital period could escape spectroscopic detection. Second, if we identify the 0.1082 day spectroscopic period with the rotation period of the white dwarf, the 0.1165 day photometric modulation is left unexplained. This interpretation must, therefore, be rejected.

c) X-Ray Observations of V795 Herculis

Rosen *et al.* (1989) report that they observed V795 Her with *EXOSAT* and failed to detect any X-ray emission. The 3 σ upper limits to the X-ray fluxes were 1.2×10^{-12} ergs cm^{-2} s^{-1} in the 0.02–2.5 keV band and 2.4×10^{-12} ergs cm^{-2} s^{-1} in the 2.5–6 keV band.

These stringent upper limits are interesting because it is generally thought that intermediate polars are strong X-ray sources. The association of strong X-ray emission with intermediate polars may, however, be partly a selection effect: Most intermediate polars are first detected by their X-ray emission and later studied at optical wavelengths, guaranteeing that they are X-ray sources. A few exceptional systems have been identified as intermediate polars or DQ Her stars at optical wavelengths before they were observed at X-ray wavelengths, usually because they show highly coherent periodic variations in their optical light curves. Limiting our list to the least controversial system, we include DQ Her itself, AE Aqr, TT Ari, and now V795 Her among these systems. The X-ray emission from all these systems is weak or undetectable. The X-ray emission from AE Aqr has been detected and its properties are particularly instructive because it is pulsed at 33 s, demonstrating conclusively that AE Aqr is a magnetic accreter (Patterson *et al.* 1980). Nevertheless, the X-ray luminosity of AE Aqr is low, 10^{31} ergs s^{-1} in the 0.1–4.0 keV range, and the X-ray emission would not have been detected if it were not among the nearest of the cataclysmic variables.

It appears that detectable X-ray emission is not a necessary concomitant of magnetic accretion and that the intermediate polars showing strong X-ray fluxes are a only a subset of the

© American Astronomical Society • Provided by the NASA Astrophysics Data System

1990ApJ...354..708S

entire class of magnetic accreters. We have no preferred explanation for the lack of strong X-ray emission from some intermediate polars, but two possibilities seem worth investigating: the X-ray could be emitted in a tight beam that misses the Earth or the X-ray spectrum could be extremely soft so that it is missed by the detectors or absorbed before reaching the Earth.

d) The Evolutionary State of V795 Herculis

V795 Her is one of the few cataclysmic variables with an orbital period lying near the middle of the gap in the distribution of periods between roughly 2 and 3 hr. There may be two ways to account for the anomalous period of V795 Her. When the system was first formed in its precataclysmic state, its secondary star may have had an unusually low mass. If so, the orbital period at which the secondary star first established contact with its Roche lobe and began mass transfer could have been much shorter than normal, possibly less than 3 hr. V795 Her would then be the descendant of a system roughly like MT Ser (Green, Liebert, and Wesemael 1984).

Alternatively, the evolution of cataclysmic variables with periods above the gap is believed to be driven by angular momentum loss due to magnetic braking (Verbunt and Zwaan 1981; Rappaport, Verbunt, and Joss 1983; Taam 1983; Patterson 1984). The rapid mass loss that results from the magnetic braking causes the secondary to depart from thermal equilibrium and to grow in radius. The degree of departure is a function of the mass-loss rate, which in turn is a function of the strength of the braking. Below a critical mass, the secondary becomes fully convective and the efficiency of the magnetic braking is diminished. It is this sudden decrease of magnetic activity when the secondary becoming fully convective that causes the system to shrink in radius, become detached, and enter the gap (Spruit and Ritter 1983).

In their discussion of V Per, which has an orbital period nearly identical to V795 Her and may also be an intermediate polar, Shafter and Abbott (1989) noted that the secondary stars in systems with low rates of mass transfer are not driven as far out of thermal equilibrium as systems with high rates of mass transfer. The period gap may be much narrower for such systems. Binaries with low transfer rates should evolve to shorter orbital periods before their secondaries becomes fully convective, narrowing the gap from the upper end. Their secondaries may also shrink less in radius and reestablish contact at longer orbital periods, narrowing the gap from the lower end. We speculate, as did Shafter and Abbott (1989) for V Per, that the mass transfer rate in V795 Her was lower than the rates in most other cataclysmic variables when it was above the period gap. It is transferring mass even though it is within the standard period gap because it is not in its own, much narrower, period gap. The dispersion in the rates of mass transfer in most cataclysmic variables above the gap appears to be small because the boundary of the gap is sharply defined. The evolutionary states of V Per and V795 Her are, therefore, most unusual.

V. CONCLUSIONS

The light curve of V795 Her varies with a period of 0.1164865(4) days. Its spectrum has a radial velocity variation with a *different* period of 0.1082648(3) days. One cycle per day aliases of the spectroscopic period can not be eliminated with absolute certainty, but the aliases are also incompatible with the photometric period. We are unable to confirm the presence of the previously reported spectroscopic period at 0.6151 days. We interpret V795 Her as an intermediate polar. We identify the 0.1082648 day spectroscopic period as the orbital period of the binary system and the 0.1164865 day photometric period as the beat period between the orbital period and the rotation period of the white dwarf. The beating is caused by reprocessing of X-rays from the poles of the white dwarf in the atmosphere of the companion star. This interpretation predicts that the white dwarf has a rotational period of either 0.065108 or 0.073907 days depending on whether radiation is being reprocessed from one or both poles of the white dwarf.

Although V795 Her has not yet been detected at X-ray wavelengths, it should have weak X-ray emission. Time-resolved X-ray observations would be extremely valuable for a complete understanding of V795 Her. It should be possible to measure the rotation period of the white dwarf directly from the X-ray light curve. Once the white dwarf rotation period has been established, it should be easy to identify the optical photometric and spectroscopic periods and to formulate a complete model for this system.

This work has been supported in part by NSF grant AST87-04382. B. W. thanks McGraw Hill Observatory for telescope time and the NSF for partial support under NSF grant AST85-15219 to G. Wegner. We thank Lu Wenxian for obtaining and reducing some of the spectra obtained at DAO. R. M. P. acknowledges the receipt of a SERC/NATO fellowship during this work.

REFERENCES

Baidak, A. V., Lipunova, N. A., Shugarov, S. Yu., Moshkalev, V. G., and Volkov, I. M. 1985, *Inf. Bull. Var. Stars*, No. 2676.
Buckley, D. A. H., and Tuohy, I. 1990, *Ap. J.*, **349**, 296.
Green, R. F., Ferguson, D., Liebert, J., and Schmidt, G. 1982, *Pub. A.S.P.*, **94**, 560.
Green, R. G., Liebert, J., and Wesemael, F. 1984, *Ap. J.*, **280**, 177.
Hutchings, J. B., Link, R., and Crampton, D. 1983, *Pub. A.S.P.*, **95**, 264.
Kaluzny, J. 1989, preprint.
Lomb, N. R. 1976, *Ap. Space Sci.*, **39**, 447.
Mardirossian, F., Mezzetti, M., Pucillo, M., Santin, P., Sedmak, G., and Giurcin, G. 1980, *Astr. Ap.*, **85**, 29.
Mironov, A. V., Moshkalev, V. G., and Shugarov, S. Yu. 1983, *Inf. Bull. Var. Stars*, No. 2438.
Nather, R. E. 1973, *Vistas Astr.*, **15**, 91.
Patterson, J. 1979, *Ap. J.*, **234**, 978.
———. 1984, *Ap. J. Suppl.*, **54**, 443.
Patterson, J., Branch, D., Chincarini, G., and Robinson, E. L. 1980, *Ap. J. (Letters)*, **240**, L133.
Press, W. H., and Rybicki, G. B. 1989, *Ap. J.*, **338**, 227.
Pritchet, C. J., Mochnacki, S., and Yang, S. 1982, *Pub. A.S.P.*, **94**, 733.
Rappaport, S., Verbunt, F., and Joss, P. C. 1983, *Ap. J.*, **275**, 713.
Robinson, E. L. 1983, in *IAU Colloquium 72, Cataclysmic Variables and Related Objects*, ed. M. Livio and G. Shaviv (Dordrecht: Reidel), p. 1.
Rosen, S. R., Branduardi-Raymont, G., Mason, K. O., and Murdin, P. G. 1988, preprint.
Scargle, J. D. 1982, *Ap. J.*, **263**, 835.
Schneider, D. P., and Young, P. J. 1980, *Ap. J.*, **238**, 946.
Shafter, A. W. 1983, *Ap. J.*, **267**, 222.
———. 1985, in *Cataclysmic Variables and Low Mass X-Ray Binaries*, ed. D. Q. Lamb and J. Patterson (Dordrecht: Reidel), p. 355.
Shafter, A. W., and Abbott, T. M. C. 1989, *Ap. J. (Letters)*, **339**, L75.
Shafter, A. W., Robinson, E. L., Crampton, D., and Warner, B. 1987, *Bull. AAS*, **19**, 1058.
Shafter, A. W., Szkody, P., Liebert, J., Penning, W. R., and Bond, H. E. 1985, *Ap. J.*, **290**, 707.
Shafter, A. W., Szkody, P., and Thorstensen, J. R. 1986, *Ap. J.*, **308**, 765.

© American Astronomical Society • Provided by the NASA Astrophysics Data System

1990ApJ...354..708S

Spruit, H. C., and Ritter, H. 1983, *Astr. Ap.*, **124**, 267.
Taam, R. E. 1983, *Ap. J.*, **268**, 361.
Thorstensen, J. R. 1986, *A.J.*, **91**, 940.
Thorstensen, J. R., Smak, J., and Hessman, F. V. 1985, *Pub. A.S.P.*, **97**, 437.
Verbunt, F., and Zwaan, C. 1981, *Astr. Ap.*, **100**, L7.
Warner, B. 1987, *M.N.R.A.S.*, **227**, 23.
Whyte, C., and Eggleton, P. 1980, *M.N.R.A.S.*, **190**, 809.

D. Crampton: Dominion Astrophysical Observatory, 5071 W. Saanich Road, Victoria, B.C. Canada V8X 4M6

R. M. Prestage: Joint Astronomy Center, Hawaii Headquarters, 665 Komohana Street, Hilo, HI 96720

E. L. Robinson: Department of Astronomy and McDonald Observatory, University of Texas, Austin, TX 78712

A. W. Shafter: Department of Astronomy, San Diego State University, San Diego, CA 92182

B. Warner: Department of Astronomy, University of Cape Town, Rondebosch 7700, South Africa

© American Astronomical Society • Provided by the NASA Astrophysics Data System